The 9th European Congress on Computational Methods in Applied Sciences and Engineering
ECCOMAS Congress 2024
3–7 June 2024, Lisboa, Portugal

ASSESSMENT OF THE ACCURACY AND ROBUSTNESS OF DIFFERENT NUMERICAL METHODS IN WALL-BOUNDED FLOWS

SIAVASH TOOSI[1], JOHAN LARSSON[2] AND PHILIPP SCHLATTER[1]

[1] Institute of Fluid Mechanics (LSTM)
Friedrich-Alexander-Universität (FAU) Erlangen-Nürnberg
91058 Erlangen, Germany
e-mail: siavash.toosi@fau.de, philipp.schlatter@fau.de

[2] Mechanical Engineering Department
University of Maryland
College Park, Maryland, 20742, USA
e-mail: jola@umd.edu

Key words: Numerical accuracy, High fidelity simulation, Wall-bounded turbulence, Finite-difference method (FDM), Spectral-element method (SEM)

Summary. Different numerical methods are tested for their accuracy and robustness in high-fidelity simulation of wall-bounded turbulent flows, on a set of 126–216 grids ranging in resolution from direct numerical simulation (DNS) to coarse wall-resolved large eddy simulation (LES). Tested numerical methods include the finite-difference discretization using second-, fourth, sixth-, and mixed-order central schemes and the spectral-element method (SEM) using different polynomial orders of 5, 7, 9 and 11. The focus is entirely on the numerical method itself, and not the specific implementation (i.e., the code; in fact, the names of the codes used for these simulations is not revealed), with the assumption that the selected methods are representative of their class of methods. To reduce bias, results are first presented using anonymized labels. The numerical method corresponding to each label is revealed after the initial conclusions about accuracy on idealistic grids.

1 INTRODUCTION

Despite the existence of a number of different approaches to spatial discretization and numerical solution of partial differential equations (PDEs), a definitive best method seems absent, at least in the context of computational fluid dynamics (CFD) in general and high fidelity simulations in particular. As a result, the choice between different methods is highly influenced by the user background and subjective experience, which is often limited and prone to bias and inaccuracies. Given the arrival of the age of exa-scale computing, the consequent increase in popularity of high fidelity simulations, and the increased amount of investment by the governments in computing infrastructure and funding to enable such simulations, it is now more important than ever to consider this question more systematically.

Several factors determine the competitiveness of a numerical method, including accuracy, robustness, cost, generality, scalability, sustainability, ease of use, and many more. In this initial

work, we are focusing entirely on accuracy and robustness. It is important to note that all these factors, including accuracy and robustness, may vary in time with new developments in the field. Here, we take an optimistic approach and assume that—with sufficient developments—all methods can be improved to achieve their nominal performance in the coming years. Therefore, we test each method is its idealistic scenario; in other words, canonical flows in simple geometries. For example, by considering a channel flow at a relatively low Reynolds number (the test case here) as a representative test case for wall-bounded flows, we are avoiding issues related to numerical dissipation (most significant at higher Reynolds numbers), performance on grids with poor quality (e.g., skewness, aspect ratio, etc.), gradient discontinuities inherent to spectral element methods, and similar, while trying to avoid factors such as inflow turbulence from impacting the results. The assumption is that by including a sufficient number of canonical flow test cases (stability, transition, shear flows, ...) one can get a picture of the ideal performance of each numerical method in high fidelity simulations. The current study in still in its early stages and only includes the turbulent channel channel flow as a representative test case for wall-bounded turbulent flows.

The final goal is to include as many numerical methods as possible. However, this initial work only includes the finite-difference and spectral-element methods.

2 METHODOLOGY

2.1 Numerical methods

Two classes of numerical methods are considered: finite-difference method (FDM) and continuous Gelerkin (CG) spectral element method (SEM).

The finite-difference scheme solves the compressible Navier-Stokes equation using a central scheme for computing the derivatives, the split form of the convective term, and a classic 4th-order Runge-Kutta method for integration in time. The dynamic Smagorinsky model (DSM) is used as the subgrid scale (SGS) model.

The CG spectral element scheme solves the incompressible Navier-Stokes equation on the Gauss-Lobatto-Legendre (GLL) points using the $P_n - P_n$ method for velocity/pressure coupling, with dealiasing of the convective term using the 3/2-rule and a third-order implicit scheme for time integration (except for the convective term, which is extrapolated using a third-order explicit scheme). The effect of unresolved scales is modeled using a high-pass filter relaxation term [1], acting on two modes with an amplitude of approximately $0.1/\Delta t$ (equivalent to 10% attenuation of the amplitude of the highest mode), where Δt is an *a priori* approximation of the time step in each simulation.

The choice of one compressible and one incompressible solver for this study was intentional, to avoid arguments related to cost comparison which could distract from our main discussion about accuracy and robustness. The differences in the setups reflect the most popular settings often used with each of the methods.

2.2 Test case

The test case is a turbulent channel flow at a bulk Reynolds number of $Re_b = U_b\delta/\nu = 10,000$, where U_b is the bulk velocity, δ is the channel half-width, and ν is the kinematic viscosity. This corresponds to a friction Reynolds number of $Re_\tau = \delta u_\tau/\nu \approx 550$, where u_τ is the friction velocity. The computational domain is a Cartesian box defined as $\Omega : (x, y, z)/\delta \in [0, 2\pi] \times$

$[-1, 1] \times [0, \pi]$, with periodic boundary conditions in the streamwise and spanwise directions, and a body force to ensure a constant mass flow rate. The upper and lower walls have no-slip and no-penetration boundary condition on the velocity field, and are considered iso-thermal in the compressible solver.

Each simulation is started from a user generated initial condition to trigger transition into turbulence, and is then integrated in time for (a conservative) $400\delta/U_b$ to discard the transients and achieve statistically stationery state. Solution statistics are collected for another $400\delta/U_b$ (around $22\delta/u_\tau$), as 200 snapshots with a temporal separation of $2\delta/U_b$ (around $0.11\delta/u_\tau$).

The domain size and averaging times are similar to those concluded by [2] to be sufficient for reproducing accurate one-point statistics.

2.3 Grid design

A total of 216 grids are generated based on a base DNS grid—with inner-scaled resolution of $(\Delta x^+, \Delta y_w^+/2, \Delta z^+) = (12.0, 0.5, 5.0)$ at the wall—by varying (coarsening) the resolution in different directions by factors of 1, 1.5, 2, 3, 4, and 5 and any possible combination of these factors (resulting in $6^3 = 216$ grids). Some numerical methods are tested on all 216 grids, some on a subset of 126 grids—including the base DNS grid and the coarsened versions by factors of 1.5, 2, 3, 4 and 5 (i.e., $1 + 5^3 = 126$)—and others somewhere in between (i.e., each method is tested on at least 126 grids). We consider the base DNS grid and the five additional isotropically coarsened ones as ideal or "design" grids. This is to acknowledge that an ideal grid would use these resolutions, or similar to them, if possible. The anisotropically coarsened grids are considered "off-design" grids, in the sense that while not ideal, in most realistic scenarios, even in quite simple geometries, they cannot be avoided. The design grids are used for assessing the (ideal) accuracy of the numerical methods, while the off-design grids are used primarily to assess their robustness. Not all 126–216 grids are used in the present work, but only a subset of around 80 grids as explained in Section 2.5.

The streamwise and spanwise resolutions of the base grid are selected as a typical academic DNS resolution for the purpose of physical studies of the flow, while perhaps not quite as fine to serve as reference data for the community. The wall-normal distribution is chosen close to a power-law distribution that has a plateau at the center: particularly, a Chebyshev distribution of 257 points (essentially the same as [3]) with its near-wall resolution being limited to $\Delta y_w^+/2 = 0.5$, followed by a smoothing step to avoid any sharp jumps in the stretching factor. The coarsened y distributions are generated by multiplying the Δy distribution of the base DNS grid by the coarsening factor and regenerating a new point distribution from the new Δy as a function of y.

Grid generation for the four finite-difference methods is quite straightforward. For the four spectral element configurations (polynomial orders of 5, 7, 9, 11), the number of *degrees of freedom* are matched with the finite-difference grids. This is equivalent to matching the average resolution (i.e., element size divided by the polynomial order) between the two methods. While the effective resolution of a GLL distribution can be a matter of debate, for the purposes of this study having the same number of degrees of freedom seems the most logical choice.

2.4 Assessment criteria

This initial study focuses on two main quantities of interest (QoIs): mean velocity and the three normal Reynolds stresses. All profiles are normalized with friction variables [4], i.e.,

$u_\tau = \sqrt{\tau_w/\rho_w}$ (where τ_w and ρ_w are shear stress and density at the wall) as the velocity scale and $\delta_\nu = \nu/u_\tau$ (also denoted by l^*) as the length scale. This helps obtain compound quantities and reduce the dependence of our conclusion to a limited set of QoIs.

The error in the QoIs is defined using the following two relations [5]:

$$|\Delta U^+| = \frac{\int_{y^+_{\min}}^{y^+_{\max}} |U^+ - U^+_{\mathrm{ref}}| \mathrm{d}\ln y^+}{\int_{y^+_{\min}}^{y^+_{\max}} \mathrm{d}\ln y^+} \tag{1}$$

$$\Sigma|\Delta R^+_{ij}| = \frac{\Sigma_{i=j=1}^{3} \int_{y^+_{\min}}^{y^+_{\max}} |R^+_{ij} - R^+_{ij,\mathrm{ref}}| \mathrm{d}\ln y^+}{\int_{y^+_{\min}}^{y^+_{\max}} \mathrm{d}\ln y^+},$$

where the lower and upper bounds of $y^+_{\min} = 5$ and $y^+_{\max} = 100$ are selected to exclude the viscous sublayer where the values always match the reference data as a property of normalization with friction units, and discard the outer region since the observed differences are primarily consequences of differences in the $y^+ \leq 100$ region. Note that taking the integrals in logarithmic scale is equivalent to having a weight function of $1/y^+$ and is done to put a higher emphasis on the near-wall region. Reference profiles, U^+_{ref} and $R^+_{ij,\mathrm{ref}}$, are taken from separate DNS results using a Fourier-Chebyshev code for the incompressible channel flow and a 6th-order finite-difference code for the compressible channel flow, both run on the same domain size as the simulations of this study but on finer resolutions than the base DNS grid used for grid design. The error in the Reynolds shear stress is already represented by the error in the mean velocity profile and is therefore not included in the definition of $\Sigma|\Delta R^+_{ij}|$.

While the error values computed from Eqn. 1 make intuitive sense, we still start by presenting the results of Section 3 by plots of the mean profiles. This is partly to get a better sense of the obtained results, and partly because some of the relative values for the errors were slightly different than what a user would conclude from the profiles.

2.5 Robustness

Robustness of the numerical methods is defined here as the change in the profile for changes in the resolutions and assessed on six resolution levels (on the six design grids). Only grids with one level up or down in resolution are considered; in other words, for the resolution level of $(\Delta x^+, \Delta y^+_w/2, \Delta z^+) = (24, 1.0, 10)$ (isotropic coarsening factor of 2) a total of 27 grids with coarsening factors of 1.5, 2, and 3—and all possible combinations of these factors in streamwise, wall-normal and spanwise direction—are considered in robustness assessment. After computing $|\Delta U^+|$ and $\Sigma|\Delta R^+_{ij}|$ from Eqn. 1 for these 27 grids, the change in the profiles is defined as the difference between the maximum and minimum values for the two errors. This is arguably not an ideal definition, since it may be prone to outliers; however, for this initial study it was deemed sufficient. Also note that considering resolutions that are only one level up or down is in fact quite optimistic (especially for coarser levels) and observed perhaps only on the most elaborately designed grids; therefore, the robustness assessments here should be viewed as the minimum requirements for a numerical method.

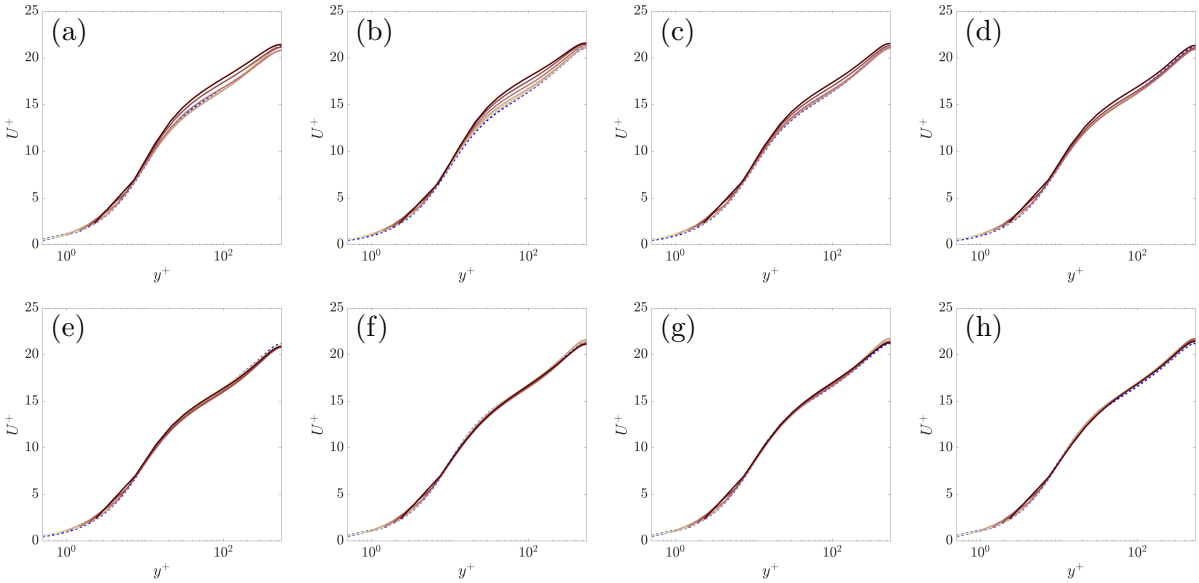

Figure 1: Mean velocity profiles for the eight numerical methods tested here. Panels (a)–(h) correspond to methods A–H. Dotted blue lines show the reference profile U^+_{ref}. Solid lines in each panel correspond to the 6 design (isotropically coarsened) grids ranging from the lightest color for the base DNS resolution (coarsening factor 1) to the darkest color for the coarsest design grid (coarsening factor 5).

3 ACCURACY

In order to reduce the bias in interpreting the results, the different methods are presented anonymously first in Section 3.1 and revealed later in Section 3.2. We strongly recommend the readers to follow the text as written and not to start Section 3.2 before concluding their thoughts on the findings of Section 3.1.

3.1 Anonymized results

The eight different numerical methods—four finite-difference solutions with different orders of accuracy and four spectral-element solutions with different polynomial orders—are labeled A–H corresponding to the panels in Figs. 1 and 2. These figures provide an overview of the relative accuracy of the different numerical methods on the ideal (design) grids over the range of resolutions considered in this study.

Method A, shown in Figs. 1 (a) and 2 (a), makes accurate predictions of the inner-scaled mean velocity up a coarsening factor of 2 (i.e., a resolution of $(\Delta x^+, \Delta y^+_w/2, \Delta z^+) = (24, 1.0, 10)$). However, for coarser grids the slope of the mean velocity profile is clearly wrong. Unfortunately, even at the DNS resolution (coarsening factor of 1) this method is incapable of producing accurate results for the Reynolds stresses, which hinders its capacity as a reliable tool for physical studies of the flow field.

Method B, shown in Figs. 1 (b) and 2 (b), offers a better performance at finer resolutions and produces accurate results for both the inner-scaled mean velocity and Reynolds stresses up to a coarsening factor of 1.5. However, for this method as well the profiles quickly diverge from the reference results at coarser resolutions.

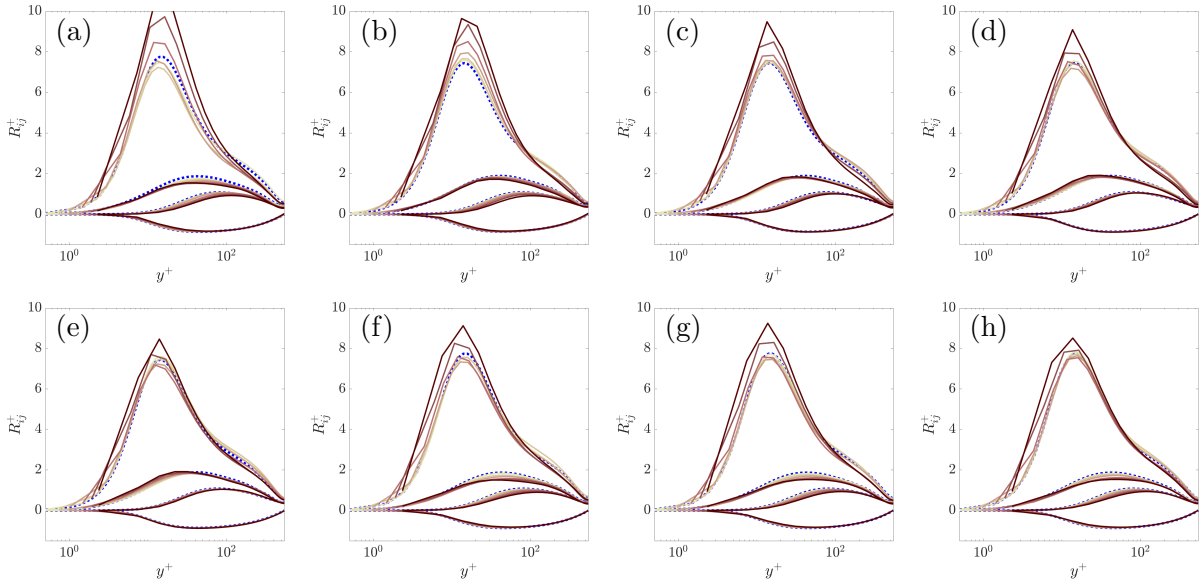

Figure 2: Reynolds stress profiles for the eight numerical methods tested here. See the caption of Fig. 1 for more details and interpretation of colors.

The inner-scaled mean velocity profile obtained from method C (Fig. 1 (c)) remains nearly indistinguishable from the reference profile up to a coarsening factor of 3, and start to diverge only at resolutions of $(48, 2.0, 20)$ or coarser. The Reynolds stress predictions of this numerical method (Fig. 2 (c)) is accurate up to a coarsening factor of 2, and somewhat acceptable at the coarsening factor of 3, i.e., a resolution of $(36, 1.5, 15)$. These profiles become inaccurate at the coarsening factor of 4 and above.

Results from methods D and E are rather sensitive to the grid resolution, even at the finer grids. This can be observed from the variations in the streamwise Reynolds stress, R_{11}^+, in Figs. 2 (d,e). In addition, these results appear to be somewhat impacted by error cancellation, seen as a decrease and then increase in the peak value of R_{11}^+, which seem to help the results remain around the reference profiles and avoid incurring large errors. While interpretation of this sensitivity can be a matter of discussion, in absolute terms, methods D and E seem to remain accurate over a larger range of scales.

Method F, shown in Figs. 1 (f) and 2 (f), makes accurate predictions for the mean velocity over the entire range of resolutions up to the coarsening factor of 5. While this method outperforms methods A–E in its mean velocity predictions, its Reynolds stress predictions are not quite as accurate and resemble a level of accuracy over this range of resolutions similar to method C (although less accurate at finer resolutions).

Method G, as evidenced by Figs. 1 (g) and 2 (g), makes accurate predictions of mean velocity for all resolutions considered, and accurate Reynolds stresses up a resolution of $(36, 1.5, 15)$. Method H performs similar to method G (compare Figs. 1 (g,h) and 2 (g,h)), while slightly improving on the accuracy of both mean velocity and Reynolds stresses. While method H outperforms all other methods in mean velocity and streamwise Reynolds stress, its underprediction of wall-normal and spanwise Reynolds stresses (R_{22}^+ and R_{33}^+) makes its overall accuracy for the Reynolds stresses more similar to method E.

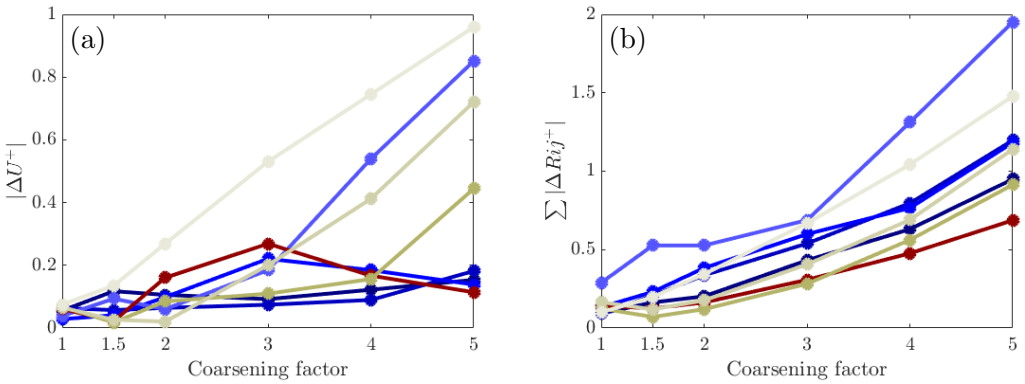

Figure 3: The error in the mean velocity (a) and Reynolds stresses (b) as a function of coarsening factor. See Table 1 for the color used for each method.

Figure 3 summarizes the results using $|\Delta U^+|$ and $\Sigma|\Delta R_{ij}^+|$ computed from Eqn. 1. The poor performance of method B in mean velocity predictions on coarser grids and method A in Reynolds stress predictions on all grids is quite obvious from the high value of the respective errors. Similarly, the error cancellations observed in method E is visually clear from an increasing trend in the error followed by a decrease.

Observations from Figs. 1, 2, and 3 are used to rank the methods based on the overall accuracy of their predictions for the inner-scaled mean velocity and inner-scaled Reynolds stresses. These ranking are done based on user judgment and by putting a higher weight on having lower errors over the range of resolutions and higher accuracy at finer resolutions. For each of the methods A–H, the two rankings are combined together by obtaining an overall rank by sorting the sum of the two rankings. These rankings are presented in Table 1. It is observed that method H offers the highest accuracy over the largest range of resolutions and is a distant winner based on this sorting method. Methods E and G are second and third, respectively, with only a small separation between them. Methods A and B are tied for the last place, and are clearly inferior choices by a large margin compared to the second to last method C (a difference of 15 compared to 10 in the sum of their rankings).

We strongly recommend the readers to take a pause here and conclude their thoughts before making to the next section where the numerical method associated to each label is revealed.

3.2 Reveal and further discussions

Correspondence between the numerical methods studied here and the labels used in Section 3.1 is revealed in Table 2. To summarize, in our results, a 6th-order finite difference method (method H) outperformed all other numerical methods by a noticeable margin, and a 4th-order finite-difference method (method G) was a close third after a CG-SEM with $p = 11$ (method E). A mixed-order finite-difference method with a 4th-order central scheme for the convective term and a 2nd-order central scheme for the diffusive term leads to the same overall accuracy as a spectral-element simulation with $p = 9$, and they are followed closely by a CG-SEM with $p = 7$. Rather surprisingly, the 2nd-order FDM and the CG-SEM with $p = 5$ lead to comparable results which are clearly inferior to all other numerical methods tested here.

It is important to note that these findings were based on the overall accuracy of the methods

Table 1: Summary of the results using anonymized labels. Color corresponds to the color used for each method in Figs. 3, 4 and 5. The overall rank of the method is obtained by sorting the sum of its ranking for mean velocity and Reynold stress predictions.

Identifier	Color	Rank: $\lvert\Delta U^+\rvert$	Rank: $\Sigma\lvert\Delta R_{ij}^+\rvert$	Sum	Total rank
A	–	7	8	15	7 (tie)
B	–	8	7	15	7 (tie)
C	–	5 (tie)	5 (tie)	10	6
D	–	5 (tie)	3	8	4 (tie)
E	–	4	1 (tie)	5	2
F	–	3	5 (tie)	8	4 (tie)
G	–	2	4	6	3
H	–	1	1 (tie)	2	1

on all six design grids, spanning resolutions from a typical DNS to a coarse wall-resolved LES. In that regard, they might be better thought of as pertaining to versatility of the methods. It is insightful to look at the performance of different methods as a function of resolution as well.

At resolutions corresponding to DNS and fine LES (coarsening factors 1 and 1.5, i.e., resolutions up to $(18, 0.75, 7.5)$), the CG-SEM methods are very accurate at all polynomial orders. The lowest polynomial order, $p = 5$, seems slightly sensitive to the resolution, and therefore $p = 7$ is arguably the best choice here for its high accuracy and lower cost. Finite-difference methods are ranked here based on their nominal order of accuracy. As was mentioned before, even at these resolutions the 2nd-order finite-difference method remains inaccurate in its predictions of the Reynolds stresses. It is also interesting to note that while a 4th-order method leads to more accurate results compared to a mixed-order formulation, the gains are not quite as significant, suggesting that the discretization of the convective term plays a more important role in determining the accuracy of the results than the viscous term.

The CG-SEM set of methods start to show some sensitivity to the grid resolution at coarsening factors 2-3 (i.e., resolutions around $(24, 1.0, 10)$ to $(36, 1.5, 15)$) corresponding to a typical wall-

Table 2: (*Please do not read before reading Section 3.1 and concluding your thoughts*) Reveal of numerical methods. See the caption of Table 1 for more details.

Method	Identifier	Color	Rank: $\lvert\Delta U^+\rvert$	Rank: $\Sigma\lvert\Delta R_{ij}^+\rvert$	Sum	Total rank
FDM: 2nd	A	–	7	8	15	7 (tie)
SEM: $p = 5$	B	–	8	7	15	7 (tie)
SEM: $p = 7$	C	–	5 (tie)	5 (tie)	10	6
SEM: $p = 9$	D	–	5 (tie)	3	8	4 (tie)
SEM: $p = 11$	E	–	4	1 (tie)	5	2
FDM: mixed	F	–	3	5 (tie)	8	4 (tie)
FDM: 4th	G	–	2	4	6	3
FDM: 6th	H	–	1	1 (tie)	2	1

resolved LES. While SEM with $p = 7$ and $p = 9$ remains accurate at these resolutions, the lowest polynomial order, $p = 5$, becomes inaccurate and the highest polynomial order, $p = 11$, starts to show some sensitivity to grid resolution in the form of error cancellation. The finite-difference method again exhibits a more uniform and predictable behavior, where the higher discretization orders lead to more accurate results.

The coarse wall-resolved LES region (coarsening factors 4-5, resolutions around $(48, 2.0, 20)$ to $(60, 2.5, 25)$) is where the CG-SEM shows its largest errors and where the FDM (with the exception of second-order) shines in its robustness of the mean velocity profile (arguably the more important QoI at these resolutions). It is important to note that at these resolutions the Reynolds stress predictions from SEM and FDM are rather comparable, and it is mainly the mean velocity predictions that are less accurate in SEM.

Based on this reasoning, the main disadvantage of the spectral-element methods appears to be at coarser resolutions. While this might suggest the inappropriateness of SEM for coarse wall-resolved LES (and by extension wall-modeled LES) we should emphasize that this might also be an artifact of the SGS models used in our comparisons. To test this, we repeated the 6th-order FDM simulations using different SGS models, including the Vreman model with model constants of $c_v = 0.03$ and $c_v = 0.07$, and without any explicit SGS model. The observation was that depending on the setup, the results can become less accurate than those from the spectral-element method, suggesting that more work is required before we can make a final conclusion about whether SEM is an appropriate tool for coarse or wall-modeled LES.

4 ROBUSTNESS

The other important question about a numerical method is its sensitivity to grid resolution. The ideal response of a numerical method to change in resolution is still a matter of discussion, since a coarser grid should indeed lead to less accurate results simply because of the lower amount of information available about the flow. Therefore a certain level of change in the results is always expected for a change in grid resolution; however, it is reasonable to assume that for relatively small (and unavoidable) changes in the resolution, one should expect only small variations in the results.

Figure 4 summarizes the sensitivity of each numerical method as a function of resolution level, assessed using the method described in Section 2.5. It is visually clear that both finite-difference and spectral-element methods exhibit a lower sensitivity and higher robustness at higher orders (order of accuracy in FDM and polynomial order in SEM). In addition, the two classes of numerical methods offer similar levels of robustness for Reynolds stresses, with the finite-difference method making slightly more robust predictions of the mean velocity. The spectral element methods are more robust compared to FDM at finer resolutions, especially the DNS and fine LES levels. This reinforces the findings of the previous section, making SEM a robust and accurate tool for physical studies into the flow.

5 CONCLUSIONS

A total of eight numerical method—including four finite-difference formulations at various order of accuracy, and four spectral element formulations at different polynomial orders—were tested for their accuracy and sensitivity over a range of resolutions from DNS to coarse wall-resolved LES in a turbulent channel flow at $Re_\tau \approx 550$. The grids were divided into two classes of

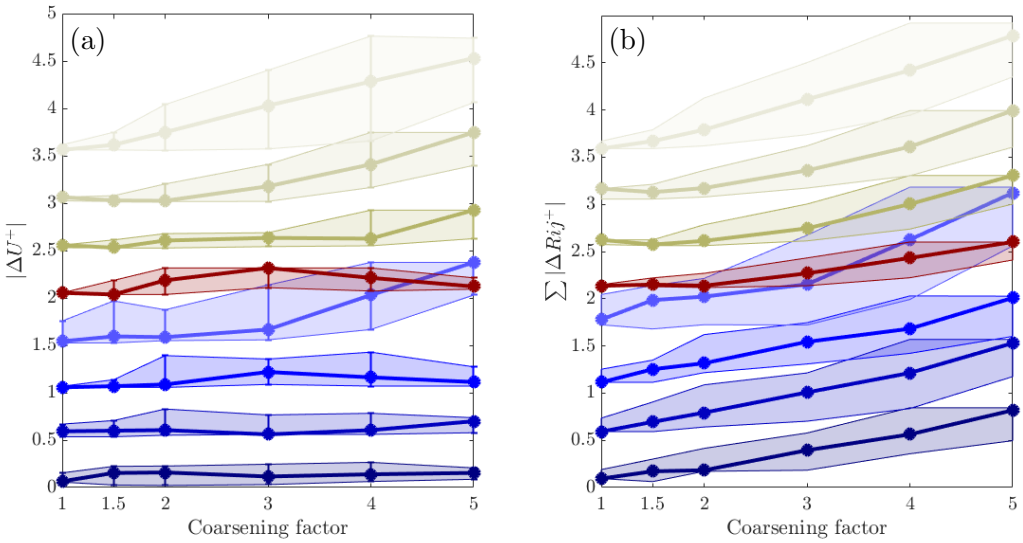

Figure 4: Error in the (a) mean velocity and (b) Reynolds stresses on the design grids (solid lines) and their sensitivity to change in grid resolution (shaded regions). Profiles are shifted vertically by 0.5 units in both panels for visual separation. See Table 1 for interpretation of the colors.

design and off-design grids, where the former was obtained by isotropic coarsening of a base DNS grid and the latter from anisotropic coarsening. A total of 216 grids were generated. However, the results presented here were obtained from a subset of around 80 grids for each numerical method; i.e., more than 600 complete simulations in total.

Our findings seem to suggest that the finite-difference method could be a more versatile choice, capable of generating accurate results over the widest range of resolutions. The major shortcominga of SEM were observed at coarser resolutions. It was argued that this might be a result of the SGS model used in SEM simulations, as has been observed before [6] As a result, the applicability of SEM for coarser simulations (such as the wall-modeled LES) remains an open question and in need of further developments before a conclusion can be drawn.

Another notable conclusion was the poor performance of the 2nd-order finite-difference method at all resolutions, including the base DNS resolution of $(12, 0.5, 5)$ (the finest resolution tested here). This was certainly unexpected to us given the popularity of the 2nd-order methods, not only in industry but in academia as well. To emphasize this point further, note that based on our results, the 4th-order finite-difference method makes more accurate predictions at a resolution of $(24, 1.0, 10)$ than the second order method at $(12, 0.5, 5)$. Even if the 4th-order method is twice as expensive as a 2nd-order simulation on the same grid (assuming being limited by MPI communication speed for instance), the 4th-order simulation is still 8 times cheaper than the 2nd-order alternative and yet leads to more accurate predictions. This has potentially substantial consequences: in particular, maybe as a community we should revisit our use of 2nd-order methods in studies of the flow physics.

We should also acknowledge the potential dependence of the conclusions on the selected QoIs. For example, if one only considers outer-scaled quantities (e.g., mean velocity profiles) they may conclude that SEM leads to more accurate and robust predictions compared to most

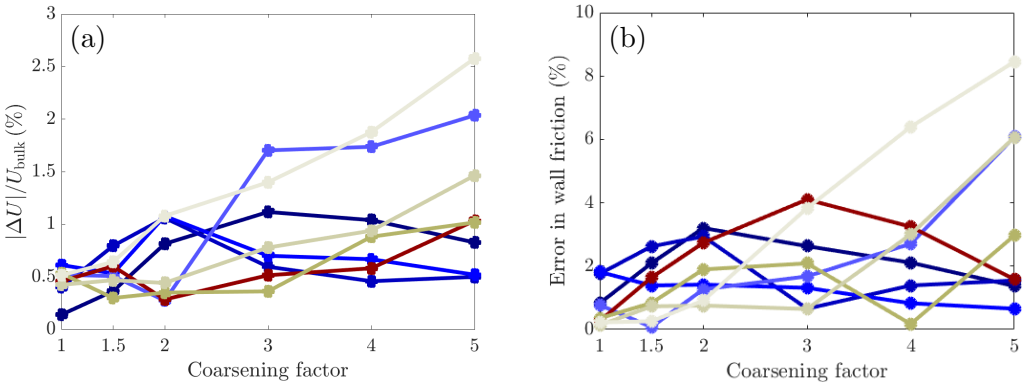

Figure 5: Comparison of error in (a) the outer-scaled mean velocity profile and (b) wall shear stress for the different numerical methods studied here.

finite-difference methods (Fig. 5 (a)). Alternatively, if one only considered the error in wall shear stress (Fig. 5 (b)) they might conclude that a 2nd-order finite-difference is sufficient, and therefore, computationally more efficient due to its lower cost. There are examples in the literature for both of these conclusions (e.g., see [7]).

The present study has a number of shortcomings to be addressed in the future. For instance, while the error definitions (Eqn. 1) were used in summarizing the results, they were not sufficiently mature to replace the user judgement based on mean flow profiles. This user judgement adds an implicit bias to the process and the conclusions. Additionally, important discussions about computational cost, algorithmic efficiency, adaptability to new architectures, and the like, were intentionally avoided here. Other factors were also not considered. These include topics related to ease of use—such as understanding the theoretical background of the method and its implementation, where the SEM has a clear disadvantage—or generality of the methods—such as the ability to easily implement new terms (e.g., a third derivative), where FDM has a disadvantage. All of these will be included in future works.

The present study should also be expanded to include additional numerical methods and test cases. The current plan includes the addition of discontinuous Galerkin (DG) spectral-element, finite-volume, and finite-element methods, and hopefully the lattice-Boltzmann method. We also envision the addition of test cases for stability and transition, wall-modeled LES, and free shear flows, with the potential for more test cases to be added later. Our final goal is to produce a database that shows the relative merits of different numerical methods and can establish a better picture of the performance and range of application of different methods, to help guide the future developments in the field. We would like to invite the community to join us in our effort to establish this database and hopefully getting a better picture of the methods with highest potential for long-term investment.

REFERENCES

[1] Schlatter P. S., S. Stolz, and L. Kleiser. 2004. "LES of transitional flows using the approximate deconvolution model." Int. J. Heat Fluid Flow 25. pp 549–558.

[2] Lozano-Durán, A., J. Jimenez. 2014. "Effect of the computational domain on direct simu-

lations of turbulent channels up to $Re_\tau = 4200$." Phys. Fluids 26, pp 011702.

[3] del Alamo, J. C., J. Jimenez. 2003. "Spectra of the very large anisotropic scales in turbulent channels." Phys. Fluids 15, no. 6, pp L41-L44.

[4] Pope, S. B. 2000. Turbulent flows. Cambridge University Press, New York.

[5] Toosi, S., J. Larsson. 2020. "Towards systematic grid selection in LES: Identifying the optimal spatial resolution by minimizing the solution sensitivity." Comp. Fluids 201. pp 104488.

[6] Rezaeiravesh, S., R. Vinuesa, P. Schlatter. 2021. "On numerical uncertainties in scale-resolving simulations of canonical wall turbulence." Comp. Fluids 277, pp 105024.

[7] Kooij, G. L., *et al.* Comparison of computational codes for direct numerical simulations of turbulent Rayleigh–Bénard convection. Comp. Fluids 166. pp 1–8.